9

A Mass Transfer Study with Electrolytic Gas Production

Eudésio O. Vilar[1], Eliane B.Cavalcanti[2] and Izabelle L.T. Albuquerque[3]
[1,3]*Federal University of Campina Grande-PB*
[2]*Tiradentes University/ITP-SE*
Brazil

1. Introduction

In general, tall vertical electrolyzers are used industrially to produce only gases like chlorine, hydrogen and oxygen, or gases and products such as soda and chlorine. Moreover, these electrolyzers usually have a very short cathode-anode distance and often operate under forced convection. For many electrochemical processes mass transfer in electrolytic cells, in particular to electrodes, must be optimized to operate economically. Many electrochemical reactions involve a gaseous component and a great deal of research has been devoted to the study of the specific features of these reactions. Three main areas have been investigated such as: the bubble formation (Chirkov & Psenichnikov, 1986), the mass transfer and hydrodynamic instabilities at gas-evolving surfaces (Kreysa & Kuhn, 1985), and the behavior of gas in porous electrodes in fuel cells (White & Twardoch, 1988). Many works were developed up to the present about gas-evolving electrodes (St-Pierre & Wragg, 1993a, 1993b; Vogt, 1979, 1984a, 1984b, 1984c, 1989a, 1989b, 1992, 1994, 1997; Czarnetzki & Janssen, 1989; Boissonneau & Byrne, 2000; Ellis et al., 1992; Janssen et al. 1984; Lastochkin & Favelukis, 1998; Wongsuchoto et al., 2002; Buwa & Ranade, 2002; Gabrielli et al., 2002; Correia & Machado, 1998; Lasia, 1998; Iwasaki et al., 1998; Fahidy & Abdo, 1982; Lasia, 1998, 1997; Barber et al., 1998; Eigeldinger & Vogt, 2000; Solheim et al., 1989; Elsner & Coeuret, 1985; Dykstra et al., 1989; Khun & Kreysa, 1989; Lubetkin, 1989; Martin & Wragg, 1989; Lantelme & Alexopoulos, 1989; Gijsbers & Janssen, 1989; Chen, 2001; Lasia & Rami, 1990; Kienzlen et al., 1994; Saleh, 1999; Janssen, 1978) but, few data on mass transfer with different cathode geometries under flow-by or flow-through electrolyte conditions with gas-evolving have been studied (Fouad & Sedahmed, 1974; Rousar et al., 1975;; Janssen & Barendrecht, 1979, Mohanta & Fahidy, 1977; Sedahmed, 1978; Sedahmed & Shemilt, 1981; Elsner & Marchiano, 1982; Albuquerque et. al., 2009). This chapter does not intend to explore in detail the mechanism during the bubbles formed electrolytically but only show an comparative study about the effect of hydrodynamic condition over mass transfer gas-electrodes for two cathodes geometries, during the hydrogen production at chlor-alkali cell by diaphragm process in laboratory scale.

2. Mass transfer

In general, it is necessary to consider three basic mechanism to the mass transfer in electrochemical systems, : migration, convection, diffusion and reaction.

Migration is the movement of charged species through the electrolyte due to a potential gradient; the current of electrons through the external circuit must be balanced by the passage of ions through the solution between the electrodes (both cations to the cathode and anions to the anode). It is, however, not necessarily an important form of mass transport for the electroactive species, even if it is charged. The forces leading to migration are purely electrostatic and, hence, do not discriminate between types of ions. As a result, if the electrolysis is carried out with a large excess of an inert electrolyte in the solution, this carries most of the charge, and little of the electroactive species Ox (oxidized specie) is transported by migration, i.e. the transport number (Bockris & Reddy,1977) O_x is low.
Convection is the movement of a species due to fluid dynamic forces. In practice, these forces can be induced by stirring or agitating the electrolyte solution or by flowing it through the electrochemical cell. Sometimes the electrode can be moved (e.g., rotating disk electrodes). When such forms of forced convection are present, they are normally the predominant mode of mass transport. By the other hand, natural convection can arises from small differences in density, temperature or gases caused by the chemical change at the electrode surface. The treatment of mass transport, highlights the differences between laboratory experiments and industrial-scale electrolysers. As is pointed out by (Pletcher & Walsh, 1993), the need in an industrial cell is only to promote the desired effect within technical and economic restraints and this permits the use of a much wider range of mass transport conditions. In particular, a diverse range of electrode-electrolyte geometry and relative movement are possible.
Diffusion and reaction. Diffusion is the movement of a species down a concentration gradient and it occurs whenever there is an electrical charge exchange at a surface. An electrode reaction (generally fast reaction) converts starting material to product, e.g.;

$$O_x + e^- \rightarrow R_{ed} \tag{1}$$

where O_x and R_{ed} are the oxidized and reduced species respectively, hence close to the electrode surface there is a (concentration) boundary layer (up to 0.01mm thick) in which the concentration of Ox is lower at the surface than in the bulk solution while the opposite is the case for R_{ed} and, hence, O_x will diffuse towards and R_{ed} away from the electrode.
Fundamental mass transport studies in industrial electrolytic cells are dependent of the fluid dynamic or by the inertial and viscous forces. This ratio is given by the well-known Reynolds number *Re,* calculated from the Equation:

$$\mathrm{Re} = \frac{\rho L \nu}{\mu} = \frac{L \nu}{\upsilon} \tag{2}$$

where p is the density of the solution, μ its dynamic viscosity, υ its kinematic viscosity, ν a mean flow velocity and L a characteristic length (for example, the length of a flat plate electrode). At higher Reynolds number, the viscous damping is no longer predominant and turbulence increase, by the other hand, any obstacles to fluid flow, or roughness in the electrolytic cell will can cause the commencement of turbulence or micro-turbulence at lower Reynolds number. In a particularly case of electrolytic cell with gas production, the Reynolds number can be obtained by the following Equation:

$$\mathrm{Re}^* = \frac{V_g.d}{A.\upsilon} \tag{3}$$

where d is the bubble detachment diameter (m), A the electrode area (m^2) and V_g is the volumetric flow rate of gas bubbles ($m^3.s^{-1}$), defined as;

$$V_g = RTj/nFP \tag{4}$$

where R (8.314 $JK^{-1}mol^{-1}$) is the gas constant, T the absolute temperature (K), j the current density of electrolysis ($A.m^{-2}$), n the estequiometric number of electrons, F the Faraday constant (96,485 $C.mol^{-1}$) and P the pressure (atm).
Natural or forced turbulence in electrolytic cells is usually advantageous since the eddies both increase mass transport of the electroactive species to the electrode surface and promote the exchange of species between the bulk solution and the boundary layer, minimizing local pH and other concentration changes due to the electrode reaction. It is not uncommon to introduce insulating nets, bars or other structural features into the cell to act as turbulence promoters. By the other hand, the morphology of the electrode surface can act as turbulence auto-promoter (e.g. mesh, reticulated metal, particulate bed, fibrous material).

2.1 Sherwood number

The Sherwood number is a measure of the rate of mass transfer, k_d , which is usually calculated in electrolytic cells from the limiting current density j_L for several cells and electrodes configurations under specific hydrodynamic conditions, i.e., the potential of the electrode is held at a value where all the electroactive species reaching the surface undergo the electrode reaction. The Sherwood number can be obtained using the relationship:

$$Sh = \frac{k_d L}{D} = \frac{j_L L}{nFC^{\infty}D} = f \left| \begin{array}{l} \text{laminar or turbulent flow} \\ \text{fluid properties} \\ \text{temperature} \\ \text{cell configuration} \\ \text{structure and active area of the electrode} \end{array} \right. \tag{5}$$

where L (m) is a characteristic dimension of the system, n the number of electrons involved in reaction, F the Faraday constant, C^{∞} the bulk concentration ($mol.m^{-3}$) of the specie electrochemically active and D ($m^2.s^{-1}$) its diffusivity. In Equation (5) the hydrodynamic condition (laminar or turbulent flow) can be evaluated by the choice of the Equation (2) or (3) and the Schmidt number by Equation (6), where it represents the relationship between the resistivity of momentum and mass diffusivities.:

$$Sc = \frac{\mu}{\rho D} = \frac{\upsilon}{D} \tag{6}$$

In general, mass transport in electrolytic cells with flow may be expressed in terms of the following expression:

$$Sh = kRe^{a}Sc^{b} \tag{7}$$

In general, to Newtonian fluids, it is assumed 0.333 for the constant b. The constants "k" and "a" many be obtained from the logarithmic linearization of equation (7). The current limiting density, j_L is generally determined from the choice of a extremely fast reaction, for

example, the electroreduction of the ferricyanide-ion in alkaline solution providing a diffusional control under various flow rate conditions. A more detailed approach on obtaining experimental current density limit may be found in specialized publications (Coeuret & Storck, 1984; Walsh, 1993; Bockris & Reddy, 1977).

2.2 The gas evolution mechanism

Gas evolution occurs on an electrode through several phenomena. The gas produced by electrochemical reactions on the electrode dissolves in the electrolyte and is transported by diffusion (boundary layer concentration) and convection towards the bulk of the solution. The mechanism of growth and detachment of bubbles from electrode surface can develops in two or three steps depending on the size and its configuration geometry- for example, perforated plate, meshes or expanded electrodes. As presented by (Gabrielli et al.,1989), the first correspond the transient step or the bubble´s radius variation with time and its depend of the electrolyte density. During the bubble growth the second step can be limited by diffusion of the dissolved molecular gas in the solution or by the kinetics of the production of the gas. When the bubble is larger than the electrode, it is assumed that the gas produced in molecular form is all transformed to the gaseous from which increases the bubble size. The last stage of the bubble evolution, i.e. its detachment from the surface, occurs when the balance between the forces which tend to maintain it on the electrode and the forces which tend to release it is broken. These various forces include the weight of the bubble, the buoyancy, the superficial tension, the pressure, the inertia and the electrostatic forces.

2.3 Electrolytic gas production from chlorine-alkali cell

The Figure 1 has shown the well-known electrolytic diaphragm process to produce chlorine and soda products (Almeida Filho et al., 2010; Abdel-Aal & Hussein, 1993; Abdel-Aal et al., 1993). The saturated aqueous sodium chloride (saturated brine) feeds the anodic

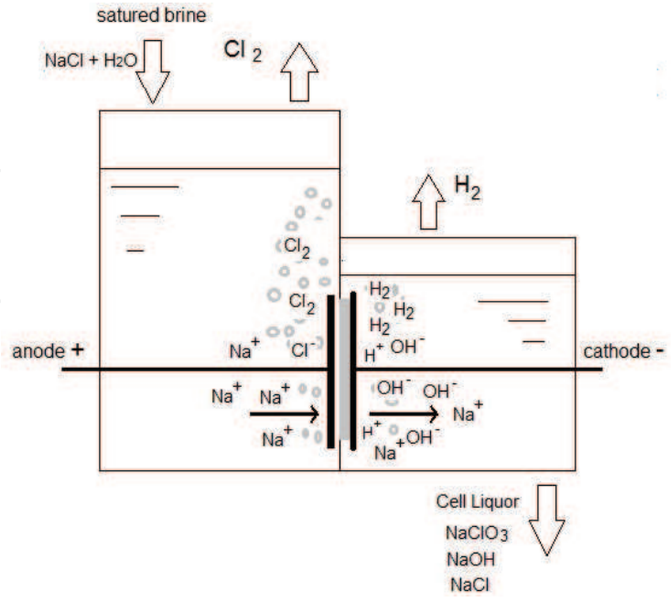

Fig. 1. Basic schematic of an electrolytic cell to produce chlorine and soda by the diaphragm process (Almeida Filho et.al, 2010)

compartment. The chlorine gas produced by the anodic reaction leaves the semi-cell, while the brine diffuses to the cathode compartment through the diaphragm due to the hydrostatic pressure drop between the two compartments. Hydrogen and hydroxyl ions are produced in the cathode compartment, which together with the sodium ions (Na^+) present in brine (anodic compartment) form sodium hydroxide (NaOH) at the same time that chlorine and hydrogen gas flow outside the cell. The part of the NaCl that did not react in the anodic compartment to produce chlorine gas diffuses into the cathode compartment through the diaphragm, joining the NaOH to form an aqueous solution of NaCl and NaOH called cell liquor.
The main reactions that occur in the process are as follows:

$$2NaCl \rightarrow 2Na^+ + Cl_2 + 2e^- \qquad \text{(anode)} \tag{8}$$

$$2H_2O + 2e^- \rightarrow H_2 + 2OH^- \qquad \text{(cathode)} \tag{9}$$

$$2Na^+ + 2OH^- \rightarrow 2NaOH + Cl_2 + H_2 \qquad \text{(global reaction)} \tag{10}$$

In the electrolytic production of chlorine-soda, high current density produces bubbles that can cover some parts of the electrode surfaces, causing an undesirable decrease in mass transfer. These limitations can be minimized through proper tuning of the cathode geometry and the electrolytic cell configuration (St-Pierre & Wragg, 1993). In industrial electrolytic operations that involve gas production, perforated plate or expanded electrodes are traditionally used to increase the reactive area per unit volume of the cell. However, the accumulation of generated bubbles on the surface of the cathode can block the electrochemically active area. This reduces efficiency by increasing ohmic drops in the layer of electrolyte adjacent to the electrode surface. Thus, the increase in the volume of bubbles adsorbed per unit area causes a decrease in mass transfer at the electrode surface (Vogt, 1984; Albuquerque, 2006, 2009). For these reasons, there has been increased interest in finding electrode geometries that promote the detachment of gas bubbles in order to increase mass transfer and ultimately efficiency.
An effective method for increasing the rate of mass transfer is to induce electrolyte turbulence near the surface to prevent the accumulation of bubbles. The behavior of this type of system was studied with expanded metal electrodes in which the electrochemical reaction on the electrode surface is controlled by diffusion and detachment of gas bubbles. (Elsner,1984) concluded that the mechanism that drives the resulting increase in mass transfer varies based on the type and orientation of the expanded metal electrode geometry and the volumetric flow direction of the electrolyte. In general, we can assume that forced convection and detachment of bubbles will improve mass transfer when the geometry of the electrode does not inhibit the release of the bubbles generated electrochemically. A strong correlation between the mass transfer coefficient and gas production has been shown in mass transfer studies. (Fouad & Sedahmed, 1973) studied this relationship for electrodes oriented vertically and horizontally, concluding that the average mass transfer coefficient is greater for horizontal electrodes. (Nishiki et al., 1987) found that generated gas bubbles decrease the conductivity between electrodes by increasing the resistance of the solution. This affected overall cell performance by increasing the potential (energy consumption of the cell). It is evident that appropriate choice of electrode material and geometry may help

to mitigate such problems. (Hine et al., 1984) studied perforated plate electrodes, concluding that variation in electrolyte resistance and overvoltage is a function of both the porosity and distance between the electrode/diaphragm interface. The porosity appears to be an important parameter for reducing the cell potential. (Jorne & Louvar, 1980) and (Jansen et al.,1984) concluded that expanded metal electrodes with a three-dimensional texture can help to prevent generated gas from accumulating on the electrode surface, thereby decreasing the ohmic drop.

3. Un example of experimental study of mass transfer with gas production

The relevance and main contribution of this study was to compare and analyze the influence of the flow perpendicular to two geometries of cathode used in electrochemical industry, on the mass transfer associated with the electrolytic production of hydrogen. The electrolytic cell used in this study is a prototype for laboratory-scale production of chlorine-soda via an electrolytic diaphragm process (see Fig. 1). The reactor has two compartments of plexiglas with 1.45 L and 0.316 L to the anode and cathode electrodes respectively, separated by an asbestos-coated diaphragm (deposited on the cathode) like shows the Fig. 2. The Fig. 3 shows the two geometric shapes to the cathode - perforated plate and mesh geometry both with 7.0 x 8.0 cm made from commercial SAE 1020 alloy. The reduction of potassium ferricyanide in alkaline medium was used for the mass transfer study with NaOH as the electrolyte support. A PAR (Princeton Applied Research)-VMP3 potentiostat, was utilized for this purpose. Table 3 lists the properties of the electrolyte solution to 27°C.

Composition	$K_3Fe(CN)_6$ = 0.005 N $K_4Fe(CN)_6$ = 0.05 N NaOH = 1.0 N
ν ($m^2.\ s^{-1}$)	0.9648×10^{-6}
D^a ($m^2.\ s^{-1}$)	6.0×10^{-10}

[a] The diffusion coefficient was calculated from the Stokes-Einstein equation: $D\mu/T=2{,}49\times10^{-15}$ [kg.m.s^{-2}.K^{-1}]

Table 3. Composition and properties of the electrolyte solution.

The reduction of potassium ferricyanide in alkaline medium was used for the mass transfer study with NaOH as the electrolyte support. A PAR (Princeton Applied Research)-VMP3 potentiostat, was utilized for this purpose. Table 3 lists the properties of the electrolyte solution to 27°C.

The experimental procedure was performed at the following conditions: volumetric flow rate between 0.03 and 0.13×10^{-3} L/s. A procedure found in the literature (Elsner,1984) was used to determine the average mass transfer coefficient with gas production. This procedure consisted of measuring the concentration variation of the reduced electroactive species ($Fe(CN)_6^{3-}$) with respect to time. The electro-reduction of ferricyanide ions in alkaline solution occurs under diffusional control. The electrochemically generated current intensity from controlled diffusion in the presence of hydrogen bubbles can then be determined from the following equation:

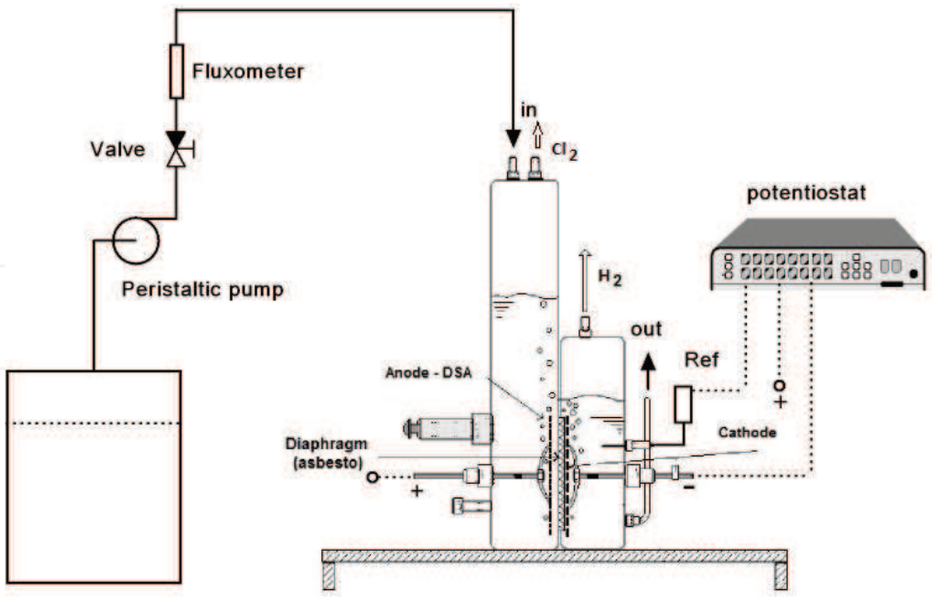

Fig. 2. Experimental set-up. Ref-reference electrode (Ni), out – soda produced (Albuquerque et. Al, 2009)

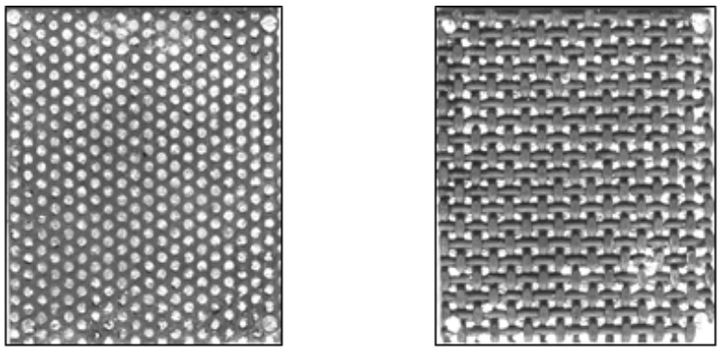

(a) (b)

Fig. 3. Cathode geometries (a) perforated plate and (b) mesh geometry.

$$j_d^g = \frac{nFV_c\Delta C}{t} \tag{11}$$

Where j_d^g (A) is the current intensity from diffusion in the presence of bubbles produced electrochemically, ΔC (mol.m^{-3}) is the gradient concentration (ferricyanide ion concentration before and after electrolysis), V_c is the volume of the cathode compartment (m^3), n is the number of electrons involved in the and t is the time of electrolysis (s). From the electrolytic current intensity, the average mass transfer coefficient was determined from the following expression:

$$\overline{k_d^*} = \frac{j_d^g}{nFA\overline{C}} \tag{12}$$

where $\overline{k_d^*}$ is the combined average mass transfer rate (m.s^{-1}), A the active area of the cathode (m^2) and $\overline{C}$ is the average concentration of ferricyanide ions during electrolysis (mol.m^{-3}). The ferricyanide concentration was determined by amperometric titration (Vilar, 1996) using a cobalt chloride (0.0339M) solution like agent in a three-electrode cell setup consisting of a Hg/HgO reference electrode, a working rotatable platinum electrode (1,000.0 rpm, 2.0 mm diameter) controlled by CTV101 speed control unit, both - Radiometer analytical and 1x1cm sheet of platinum as counter electrode. The experimental setup was controlled by potentiodynamic technique using a PAR (Princeton Applied Research)-VMP3 Potentiostat.

3.1 Modeling

The following correlation was determined to best represent the chlorine-soda electrochemical reactor used in the present work (Zlokarnik, 2002):

$$\overline{Sh} = aRe^b Sc^{1/3} = \frac{\overline{k_d^* L}}{D} = a\left(\frac{\upsilon L}{\nu}\right)^b \left(\frac{\nu}{D}\right)^{1/3} \tag{13}$$

where L (the characteristic dimension) is given by the following relationship between the porosity of the electrode ε and the specific area A_s (m^{-1}):

$$L = \frac{\varepsilon}{A_s} \tag{14}$$

and

$$A_s = \frac{A_g}{V_s} \tag{15}$$

where ε is the porosity (0.51 and 0.75 to perforated plate and mesh geometry respectively) Ag is the geometric area (57.0x10^{-4}m^2 both), and Vs the volume of solid electrode.

3.2 Results and discussion

Figure 4 shows the effect of the percolation rate of electrolyte through the diaphragm on the average mass transfer coefficient. The percolation rate (m.s^{-1}) was calculated as the ratio between the feed flow and the open cathode area (0.00287 m^2 for perforated plate and 0.0042 m^2 for mesh geometry).

It can be observed in Figure 4 that for the perforated plate geometry, the combined average mass transfer coefficient decreases with increasing percolation rate of electrolyte. The opposite behavior is observed for the mesh geometry. There are also two distinct regions in both curves, highlighted by the inflection points. This is characteristic of areas of hydrodynamic transition phenomena, probably due to laminar flow with rippling. Figure 5 helps to describe this behavior. The geometric influences are illustrated by the vector velocity of percolation (black arrows) and the direction of micro-convection (white arrows) caused by the rise of the bubbles. For the perforated plate geometry, Figure 5 (A) and (B) illustrates the supposition that the layer of micro-convection caused by the rise bubbles is pushed away from electrode surface when the cross-percolation velocity of electrolyte is

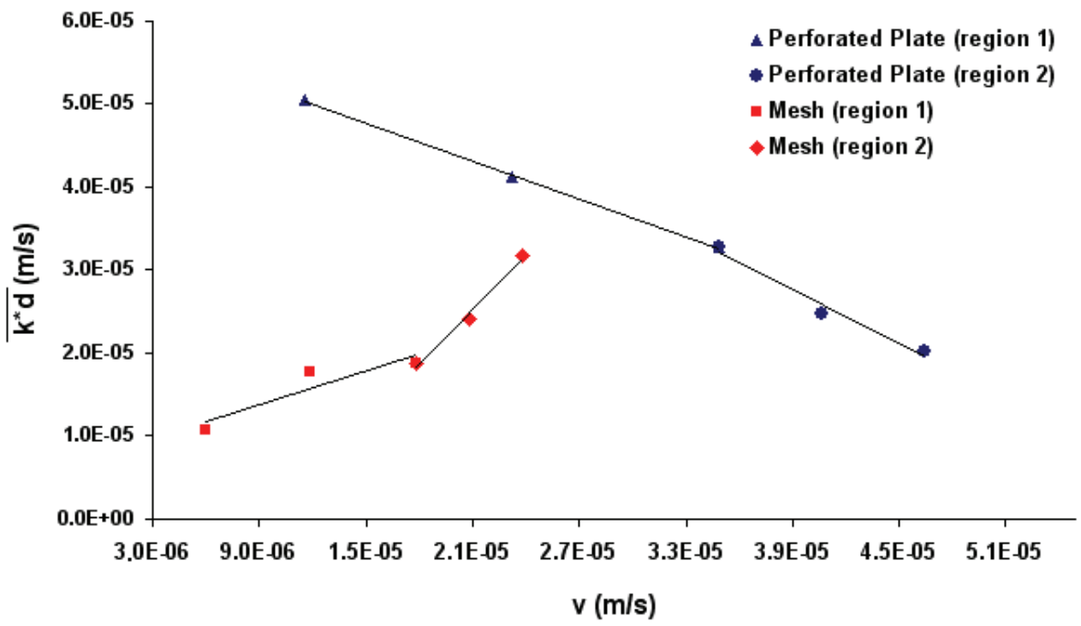

Fig. 4. Combined average mass transfer coefficient with respect to percolation rate of electrolyte.

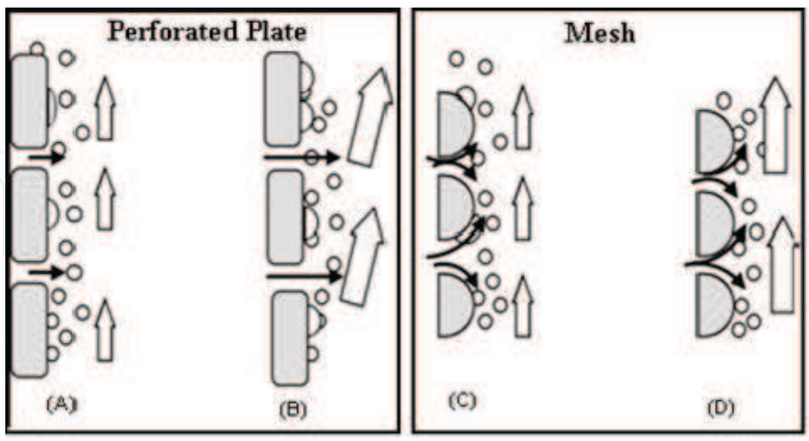

Fig. 5. Hypothesis of the situation between the change of cross-velocity percolation vectors with the rise of bubbles for; -Perforated plate, (A) -low and (B) - high velocities, -Mesh geometry, (C) -low and (D) - high velocities.

increased. This phenomena can hinder the detachment of the bubbles adhered to the cathode surface, causing a decrease in the rate of mass transfer with increasing percolation velocity. For the mesh geometry, a contrary phenomenon is illustrated. The Figure 5 (C) and (D) illustrates the same vector representation, but in this case the curved surface promotes increasing the velocity in the Prandtl hydrodynamic layer (Coeuret & Storck, 1984; Walsh, 1993), which enhances the detachment of gas bubbles. The increasing turbulence facilitates the detachment of the bubbles and the micro-convective movement reduces the Nernst boundary layer, and thereby increases the combined average mass transfer coefficient.

The Figure 5 can be explained by the supposition that turbulence can be more pronounced at the surface of the mesh electrodes than the surface of the perforated plate electrodes. For the mesh geometry, this mechanism is more significant at high percolation rates (see region 2 of Figure 4). Furthermore, this result indicates that for low percolation rates, the turbulence caused by micro-convection is not strong enough to detach the bubbles trapped in the mesh holes. This is probably due to greater bubble surface adhesion in this geometry.

With respect to dimensionless correlation, the constants a and b were determined from logarithm function applied to Equation (13). The results are shown in Figure 6 and the Table 4 list all the correlations and Reynolds numbers domains studied in this study.

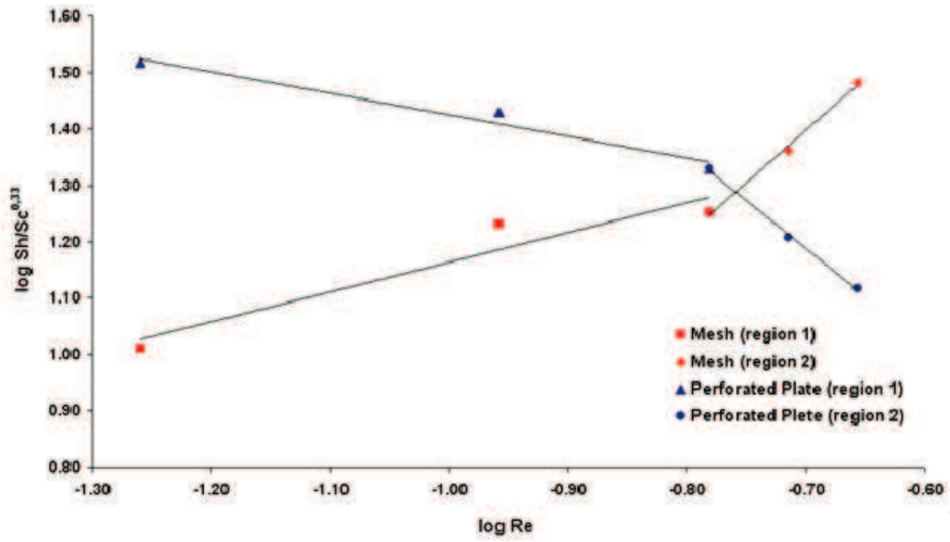

Fig. 6. The relationship between log ($Sh/Sc^{1/3}$) and log Re for mesh and perforated plate cathode geometries.

	Mesh	Perforated Plate	Reynolds
Region			
1	$\overline{Sh} = 11.01\,\mathrm{Re}^{0.38}.Sc^{1/3}$	$\overline{Sh} = 49.11\,\mathrm{Re}^{0.53}.Sc^{1/3}$	0.055<Re<0.165
2	$\overline{Sh} = 486.41\,\mathrm{Re}^{1.84}.Sc^{1/3}$	$\overline{Sh} = 1.01\,\mathrm{Re}^{-1.70}.Sc^{1/3}$	0.165<Re<0.220

Table 4. Empirical correlations for both geometries and Reynolds number domains studied.

These correlations were compared with those found in the literature. (Stephan & Vogt, 1974) proposed a model expressed by Equation (17), which correlates the mass transfer in various systems with gas evolution. This model was evaluated for 32 experiments, as shown in Figure 7.

$$Sh = \frac{\overline{k_d^*}.d}{D} = \frac{3.385}{C_\phi^{0.33}}\left(Re^* Sc\right)^{0.487}\left(1-\theta\right)^{0.5} \quad (17)$$

where d is the bubble detachment diameter (d = 40 μm for bubbles of hydrogen in alkaline solution), θ is the fraction of area covered (θ = 0.2 for semi-spherical bubbles and 0.3 for spherical bubbles) and C_ϕ is the sphere diameter (C_ϕ= 8 for bubble and 4 semi-spherical bubbles). The Reynolds number Re^* was determined by Equations (3) and (4) and the combined average mass transfer rate, k_d^* by Equation (12). The results of the present study were compared with the experimental data compiled by (Stephan & Vogt, 1974) as shows by the Figure 7. These data were obtained from acidic or alkaline solutions using various electrode materials such as platinum, copper and graphite. The data are valid for the following domain: 0^o C < T < 80°C; 3 A.m^{-2} < j <10^5 A.m^{-2} ; 160.00 < Sc < 23,000.00 and 3.0 10^{-6} < Re* < 9.0x10^{-1}

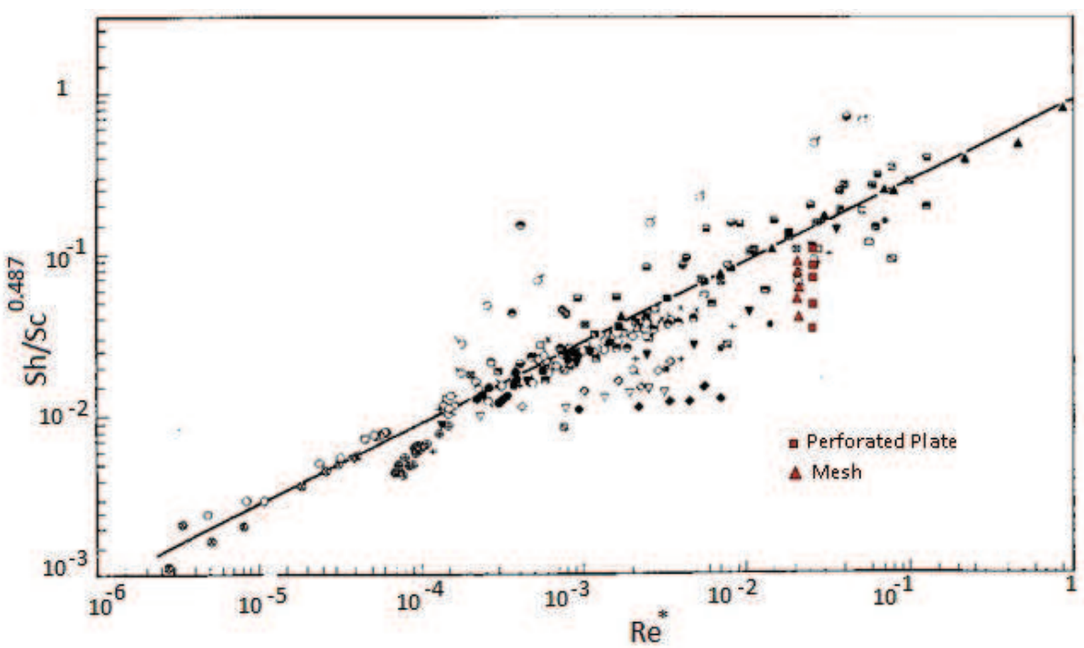

Fig. 7. Comparison of the experimental data of mass transfer with gas production (Stephan & Vogt, 1974) and the experimental data from this study.

According to Equations (3) and (4), the value of the Reynolds number is related to both the bubble velocity and the current density. For the purpose of comparison, only current density was used in this work so there is only one value of the Reynolds number.

4. Conclusions

It was shown that the mechanism controlling the average combined mass transfer coefficient during hydrogen production in electrochemical processes is dependent on the electrode geometry. The perforated plate geometry with deposited asbestos showed a slight advantage, compared with the mesh geometry, due to the detachment of bubbles from the active surface at low percolation velocities. Furthermore, increasing the percolation velocity resulted in a decrease of the average mass transfer coefficient, due to displacement of the micro-convective layer away from the electrode surface. For the mesh geometry, increasing the percolation velocity leads to an increase in the average mass transfer due to combined micro-convective effects. Specifically, rising bubbles associated with increased flow velocity over the curved wire surface, contribute to the displacement of bubbles blocked by adhesion. Finally for the chlorine-soda diaphragm process, a particularly operational industrial condition utilizing a percolation rate between 5.32 10^{-6} and 6.16 10^{-6} $m.s^{-1}$, the present study showed that the perforated plate geometry is plus advantageous.
To improve the electrochemical cells with electrolytic gas production it is very important for the mass transfer researches with new electrodes materials and geometries for cathodes and/or anodes. Thus it may be possible to achieve low energy consumption in a high efficiency process and low residues production.

5. References

Abdel-Aal, H.K & Hussein, I.A. (1993), Parametric study for saline water electrolysis: Part I-Hydrogen production, *International Journal of Hydrogen Energy,*18,6,pp.485-489.

Abdel-Aal, H.K; Sultant, S.M. & Hussein, I.A. (1993), Parametric study for saline water electrolysis:Part II-Chlorine evolution, selectivity and determination, *International Journal of Hydrogen Energy,*18,7,pp.545-551.

Albuquerque, I. L. T. (2006); Influence of cathode geometry on the mass transfer and cathode potential during the water electrolysis in alkaline environment, MsC, Federal University of Campina Grande-PB, Brazil.

Albuquerque, I.L.T.; Cavalcanti, E.B. & Vilar, E.O. (2009), Mass transfer study of electrochemical processes with gas production, *Chemical Engineering and Process: Process Intensification,*48,pp.1432-1436.

Almeida Filho, E.M.; Vilar, E.O. & Feitoza, A.C.O. (2010), Phisical-chemical characterization and statistical modeling applied in a chlor-alkali diaphragm-cell process, *Chemical Engineering and Design,* article In press, doi: 10.1016/j.cherd.2010.08.007.

Barber, J.; Morin, S. & Conway,B.E. (1998), Specificity of the kinetics of H_2 evolution to the structure of single-crystal Pt surfaces, and the relation between opd and upd H, *Journal of Electroanalytical Chemistry,* 446, pp.125–138.

Bockris, J.O'M. & Reddy, A.K.N. (1977), *Modern Electrochemistry*, Vol.1, Plenum Press/Rosetta Edition, New York.

Boissonneau, P.& Byrne P. (2000) An experimental investigation of bubble – induced free convection in a small electrochemical cell, *Journal of Applied Electrochemistry*, 30, pp. 767-775.

Buwa, V. V. & Ranade,V. V. (2002), Dynamics of gas–liquid &ow in a rectangular bubble column: experiments and single/multi-group CFD simulations, *Chemical Engineerign Science*, 57,pp.4715-4736.

Chen, Wein-X.(2001), Kinetics of hydrogen evolution reaction on hydrogen storage alloy electrode in alkaline solution and effects of surface modification on the electrocatalytic activity for hydrogen evolution reaction, *International journal of Hydrogen Energy,* 26, pp.603-608.

Chirkov, Yu.G. & Psenichnikov, A.G. (1986). 37th Meeting of the International Society of Electrochemistry, *Soviet Electrochem.*,21,114,p.283, August (1986), USSR, Vilnius

Coeuret, F. & Storck, A. (1984) *Elements de genie electrochimique*, Tec. & Doc. Lavoisier, Paris, France.

Correia, A.N. & Machado, A.S. (1998), Hydrogen evolution on electrodeposited Ni and Hg ultramicroelectrodes, *Electrochimica ActaI,*43,3-4, pp. 367-373.

Czanetzki, L.R. & Janssen, L.J.J. (1989), Electrode current distribution in a hypochlorite cell, *Journal of Applied Electrochemistry,*19,pp.630-636.

Dykstra, P.A.; Kelsall, G.H.; Liu, X. & Tseung, A.C.C. (1989), New electrodes for oxygen evolution in acidic solution, *Journal of Applied Electrochemistry,* 19,pp.697-702.

Eigeldinger, J. & Vogt, H. (2000), The bubble coverage of gas-evolving electrodes in a flowing electrolyte, *Electrochimica Acta,* 45,pp.4449-4456.

Ellis, K.A.; Fahidy, T.Z.& Pritzker, M.D. (1992) Application of computer vision to bubble detection at a gas-evolving electrode, *Chemical Engineerig Science*, 47, 13/14, pp.3623-3630.

Elsner, C. & Marchiano, S.L. (1982) The effect of electrolytically formed gas bubbles on ionic mass transfer at a plane vertical electrode, *Journal of Applied Electrochemistry*, 12, pp. 735-742.

Elsner, C.; (1984) Transfert de matière et distribution du potentiel et du courant sur des électrodes de métal deployé, en présence de bulles électro-engendrées, Cap. IV, Dr. Thesis, ENSCR, Université de Rennes I, France.

Elsner, C. & Coeuret, F., (1985), Potential distribution along gas evolving electrodes, *Journal of Applied Electrochemistry,*15,4,pp.567-574

Fahidy, T. Z. & Abdo, S. E. (1982), On the induction time of the electrolytic evolution of hydrogen bubbles, *Electrochimica Acta,* 27,10,pp.1521-1523.

Fouad, M.G. & Sedahmed, G.H. (1973), Mass transfer at horizontal gas-evolving electrodes, *Electrochimica Acta*, 18, pp. 55-58.

Fouad, M.G. & Sedahmed, G.H. (1974), Mass transfer at cylindrical gas evolving electrodes, *Electrochimica Acta*, 19, p.861

Gabrielli, C.; Huet, F.& Nogueira, R.P. (2002), Electrochemical impedance of H_2-evolving Pt electrode under bubbleinduced and forced convections in alkaline solutions, *Electrochimica Acta,* 47, pp.2043-2048.

Gabrielli, C; Macias, A.;Keddam, M.; Huet, F. &. Sahar, A. (1989), Potential drops due to an a gas-evolving electrode, *Journal of Applied Electrochemistry*, 19, pp. 617-629.

Gijsbers, H.F.M. & Janssen, L.J.J. (1989), Distribution of mass transfer over a 0.5-m-tall hydrogen-evolving electrode, *Journal of Applied Electrochemistry,*19, pp. 637-648.

Hine, F.; Yasuda, M.; Ogata, Y. & Hara, K. (1984) Hydrodynamic studies on a vertical electrolyzer with gas evolution under forced circulation, *Journal of Electrochemistry Society*, 83, p. 131.

Iwasaki, A.; Kaneko, H.; Abe, Y. & Kamimoto, M. (1998), Investigation of electrochemical hydrogen evolution under microgravity condition, *Electrochimica Acta*,46,5-6,pp.509-514.

Janssen, L.J.J.; Sillen C.W.M.P.; Barendrecht, E. & Stralen, S.J.D.(1984) Bubble behaviour during oxygen and hydrogen evolution at transparent electrodes in KOH solution, *Electrochimica Acta*, 29, pp. 630 – 642.

Jassen, L.J.J. (1978), Mass transfer at gas evolving electrodes, *Electrochimica Acta,*23,p.81

Jassen, L.J.J. & Barendrecht, E.(1978), The effect of electrolytic gas evolution on mass transfer at electrodes, *Electrochimica Acta,*24,p.735

Jorne, J. & Louvar, J.F. (1980) Gas diverting electrodes in the chlor-alkali membrane cell. Journal of Electrochemistry Society, 2, p.127.

Kienzen, V.; Haaf, D. & Schnurnberger, W. (1994), Location of hydrogen gas evolution on perforated plate electrodes in zero gap cells, *International Journal of Hydrogen Energy,* 19,9,pp.729-732.

Kreysa, G. & Kuhn, M. (1985), *Journal of Applied Electrochemistry*, 15, p.283.

Khun, M. & Kreysa, G. (1989), Modelling of gas-evolving electrolysis cells. II Ivestigarion of the flow field around gas-evolving electrodes, *Journal of Applied Electrochemistry,* 19, pp.677-682.

Lantelme, F. & Alexopoulos, H. (1989), Role of gas bubbles adsorbed on a carbon electrode: electroreduction of chlorine gas in fused salts, *Journal of Applied Electrochemistry,* 19,pp.649-656.

Lasia, A. (1998), Hydrogen evolution:oxidation reactions on porous electrodes, *Journal of Electroanalytical Chemistry*, 454, pp.115-121.

Lasia, A. (1997), Porous electrodes in the presence of a concentration gradient, *Journal of Electroanalytical Chemistry,* 428,pp.155-164.

Lasia, A. & Rami, A. (1990), Kinetics of hydrogen evolution on nickel electrodes, *Journal of Electroanalytical Chemistry,* 294, pp.123-141.

Lastochkin, D. & Favelukis, M. (1998) Bubble growth in a variable diffusion coefficient liquid, *Chemical Engineering Journal*, 69, pp.21-25.

Lubetkin, S.D. (1989), Measurement of bubble nucleation rates by an acoustic method, *Journal of Applied Electrochemistry,* 19, pp.668-676.

Martin, A.D. & Wragg, A.A. (1989), The vertical distribution of current in a gas-evolving membrane cell, *Journal of Applied Electrochemistry,*19,pp.657-667.

Mohanta, S. & Fahidy, T.Z. (1977), The effect on anodic bubble formation on cathodic mass transfer under natural convection condition, *Journal of Applied Electrochemistry,*7,p.235

Nishik, Y. i, K.; Tokuda, Aoki, K. & Matsuda, H., (1987) Current distribution in a two-dimensional narrow gap cell composed of a gas evolving electrode with an open part, *Journal of Applied Electrochemistry*, 17, pp. 67-76.

Pletcher, D. & Walsh, F.C. (1993), *Industrial Electrochemistry*, 2ªedition, Black Academic & Professional, Chapman&Hall, London.

Rousar, I.; Kacin, J.; Lippert, E.; Smirous, F. & Cezner, V. (1975), Transfer of mass or heat to an electrode in the region of hydrogen evolution II. Experimental verification of mass and heat transfer equations, *Electrochimica Acta,*20,p.295

Sedahmed, G.H. (1978), Mass transfer enhancement by the counter electrode gases in a new cell design involving a three-dimensional gauze electrode, *Journal of Applied Electrochemistry,*8,p.399

Saleh, M.M. (1999), Mathematical modelling of gas evolving flow-through porous electrodes, *Electrochimica Acta,*45,pp.959-967.

Solheim, A.; Johansen, S.T.; Rolseth, S. & Thonstad, J. (1989), Gas induced bath circulation in aluminium reduction cells, *Journal of Applied Electrochemistry,* 19,pp.703-712.

Stephan, K. & Vogt, H. (1979) A model for correlating mass transfer data at gas evolving electrodes, *Electrochimica Acta*, 24, pp. 11-18.

St-Pierre, J. & . Wragg, A.A, (1993a) Behaviour of electrogenerated hydrogen and oxgen bubbles in narrow gap cells–Part I. Experimental, *Electrochimica Acta*, 38, 10, pp. 1381–1390.

St-Pierre, J. & . Wragg, A.A, (1993b) Behaviour of electrogenerated hydrogen and oxgen bubbles in narrow gap cells–Part II. Application in chlorine production, *Electrochimica Acta*, 38, 13, pp. 1705–1710.

Vilar, E.O. (1996) Transfer de matière entre um fritté métallique et un liquid – application aux electrodes poreuses percolées. Dr. Thesis, ENSCR, Université de Rennes I, France.

Vogt, H. (1979), On the supersaturation of gas in the concentration boundary layer of gas evolving electrodes, *Electrochimica Acta,*25,pp.527-531.

Vogt, H. (1984a) The rate of gas evolution at electrodes – I. An Estimate of efficiency of gas evolution of the basis of bubble grwth data, *Electrochimica Acta*, 29,2, pp.175 - 180

Vogt, H. (1984b), The rate of gas evolution at electrodes – II. An Estimate of efficiency of gas evolution from the supersaturation of electrolyte adjacent to a gas-evolving electrode, *Electrochimica Acta*, 19, pp. 167 – 173.

Vogt, H. (1984c) Studies on gas-envolving electrodes: The concentration of dissolved gas in electrolyte bulk, *Electrochimica Acta,* 30,2,pp.265-270.

Vogt, H. (1997), Contribution to the interpretation of the anode effect, *Electrochimica Acta*, 42,17,pp.2695-2705.

Vogt, H.(1989a), The problem of the departure diameter of bubbles at gas-evolving electrodes, *Electrochimica Acta,* 34,10, pp.1429-1432.

Vogt, H. (1989b), Mechanism of mass transfer of dissolved gas from a gas-evolving electrode and their effect on mass transfer coefficient and concentration overpotential, *Journal of Applied Electrochemistry,*19,pp.713-719.

Vogt,H.(1992) The role of single-phase free convection in mass transfer at gas evolving electrodes – I. Theoretical, *Electrochimica Acta*, 28, pp. 1421-1426.

Vogt,H. (1994) The axial hypochlorite distribution in chlorate electrolyzers, *Electrochimica Acta,*39,4,pp.2173-2179.

Walsh,F. (1993) *A first course in electrochemical engineering*, The Electrochemical Consultancy, Romsey, England.

White, S.H. & Twardoch, U.M.(1988), *Journal of Electrochemical Society*, 135, p. 893.

Wongsuchoto, P.; Charinpanitkul,T. & Pavasant, P. (2003), Bubble size distribution and gas–liquid mass transfer in airlift contactors, *Chemical Engineering Journal,* 92, pp. 81-90.

Zlokarnik, M. (2002) *Scale-up in Chemical Engineering*, Wiley-VCH Verlag GmBH & Co. KGaA ISBNs: 3-527-30266-2 (Hardback); 3-527-60056-6 (Electronic).

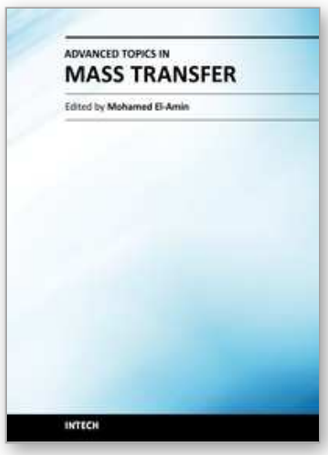

Advanced Topics in Mass Transfer

Edited by Prof. Mohamed El-Amin

ISBN 978-953-307-333-0
Hard cover, 626 pages
Publisher InTech
Published online 21, February, 2011
Published in print edition February, 2011

This book introduces a number of selected advanced topics in mass transfer phenomenon and covers its theoretical, numerical, modeling and experimental aspects. The 26 chapters of this book are divided into five parts. The first is devoted to the study of some problems of mass transfer in microchannels, turbulence, waves and plasma, while chapters regarding mass transfer with hydro-, magnetohydro- and electro- dynamics are collected in the second part. The third part deals with mass transfer in food, such as rice, cheese, fruits and vegetables, and the fourth focuses on mass transfer in some large-scale applications such as geomorphologic studies. The last part introduces several issues of combined heat and mass transfer phenomena. The book can be considered as a rich reference for researchers and engineers working in the field of mass transfer and its related topics.

INTECH
open science | open minds

InTech Europe
University Campus STeP Ri
Slavka Krautzeka 83/A
51000 Rijeka, Croatia
Phone: +385 (51) 770 447
Fax: +385 (51) 686 166
www.intechopen.com

InTech China
Unit 405, Office Block, Hotel Equatorial Shanghai
No.65, Yan An Road (West), Shanghai, 200040, China
中国上海市延安西路65号上海国际贵都大饭店办公楼405单元
Phone: +86-21-62489820
Fax: +86-21-62489821

IntechOpen